Research Square

Preprints are preliminary reports that have not undergone peer review.
They should not be considered conclusive, used to inform clinical practice,
or referenced by the media as validated information.

Investigating the environmental response mechanisms of urban basin to reclaimed water system: A case study in Northeast China

Qiuyi Ge
Hohai University
gongjin Zhang
Nanjing Hydraulic Research Institute
chengli Zhu
clz@hhu.edu.cn

Hohai University
Xing Huang
Hohai University
Shiwen Zhao
Nanjing Hydraulic Research Institute
Genxiang Feng
Hohai University

Research Article

Keywords: Reclaimed water, Urban basin, Environmental factors, Response mechanism, Northeast China

Posted Date: October 27th, 2026

DOI: https://doi.org/10.21203/rs.3.rs-10964071/v1

License: This work is licensed under a Creative Commons Attribution 4.0 International License.
Read Full License

Additional Declarations:
No competing interests reported.

Tables 1 and 2 are available in the Supplementary Files section.

Investigating the environmental response mechanisms of urban basin to reclaimed water system: A case study in Northeast China

Qiuyi Ge[a,c], Gongjin Zhang[b],Chengli Zhu[a]*, Xing Huang[a] Shiwen Zhao[b,c] Genxiang Feng[a]

[a] *College of Agricultural Science and Engineering, Hohai University, Nanjing 211100, China*

[b] *Nanjing Hydraulic Research Institute, Nanjing 210029, China*

[c] *Nanjing Hydraulic Research Institute R&D Tech Group Co.,Ltd, Nanjing 210029, China*

*Corresponding author

E-mail address: clz@hhu.edu.cn

ABSTRACT

Reclaimed water (RW) replenishment is an effective approach to addressing regional water scarcity in river basins; however, such artificial interventions significantly influence the basin environment. This study investigates the environmental response mechanisms in the Hejiagou (RHJ) River Basin in Harbin, a typical water-scarce city in Northeast China, under RW replenishment. Through in-situ monitoring from 2021 to 2024, MIKE21 modeling simulations, and statistical analysis, this study explores the basin's environmental response mechanisms under RW replenishment. The results indicate that RW recharge increased channel storage capacity by 34.62%. During non-frozen periods and when water shutdown conditions were not present, flow rates stabilized at 2~3m³/s, with velocities exceeding 2.5 m/s. Fluctuations in discharge water quality emerged as the primary factor influencing downstream river segments,

with seasonal and spatial variations determining differential quality levels across different reaches. The physical, chemical, and biological properties of sediments and microorganisms downstream of the discharge point were highly correlated with water quality. Long-term discharge and scouring elevated the downstream riverbed by 0.5~1.0m, with an average scour depth of 0.9m/a. Hydrodynamic simulations revealed substantial impacts of the discharge point on all river segments. Recommendations for strategies, such as wastewater treatment plant upgrades and dredging, provide scientifically grounded guidance for mitigating similar environmental issues in catchment areas.
Keywords: Reclaimed water；Urban basin；Environmental factors；Response mechanism；Northeast China

1. Introduction

Water is an essential natural resource for nations all over the world, and many big countries face serious problems due to regional shortages and unequal distribution （He et al., 2021）. Reclaimed water, an unusual water resource, provides a somewhat steady supply and manageable quality, thereby minimizing ecological harm, water pollution, and regional water scarcity while lowering reliance on and overuse of natural water sources (Foglia et al., 2023, Hou et al.,2020). One of the main strategies for SDG 6 that UN-Water has suggested is to "significantly increase the reuse of safe recycled water globally by 2030."(CBAS. 2025) China, a huge country with a dense population, faces comparable serious water problems. The government has prioritized the use of RW over the last five years, as evidenced by the successive policy documents it has released(Ding et al.,2022), including the《Guiding Opinions on Strengthening the Allocation and Utilization of Unconventional Water Sources》and the《Guiding Opinions on Promoting the Resourceful Utilization of Sewage》" Therefore, over the past ten years, a lot of research has been done to promote wastewater resource usage, optimize water resource allocation frameworks,

and conserve aquatic ecosystems, especially in water-scarce Northeast China（Zhang et al.,2012）. These endeavors have also shown several difficulties.

Harbin City is Northeast China's northernmost province capital, situated between 44°04′ and 46°40′ north latitude. With an annual precipitation of 545.7 mm and a long-term average temperature of 3.5°C, it is home to 32% of the province's population. The temporal distribution of water resources is irregular; external water inflows from June to August make up 60~70% of the yearly volume, which is not well matched with periods of peak production demand. Just 1.8% of all water produced by humans is used for ecological and environmental objectives. It is one of the top 10 water-scarce cities in China, with per capita water resources of 1223 m^3, or 50% of the national average and 12.5% of the global average. Three ditches, two streams, and one river make up the urban drainage system. The main outputs from the combined sewer system into neighboring rivers are sewage, snowmelt, and collected rainwater. RHJ Basin, one of the city's four rivers under study, has traditionally seen seasonal dry spells, localized water stoppages, and water pollution due to these topographical, historical, and developmental circumstances. The local government started RW utilization strategy in 2011 to solve these problems. Through this program, treated wastewater from five wastewater treatment facilities was routed to different locations along the river and ditches. Two more picturesque water replenishment locations were then added, taking into account ecological water requirements and urban landscaping (Song et al., 2024). Long-term implementation has gradually shown detrimental effects on basin water quality, channel morphology, sedimentation, hydrological conditions, and river ethics, even though these RW replenishment projects initially showed notable benefits for urban aesthetics, blue-green spaces, and flood control during their early operational phases (Sun et al.,2023). The focus of our research, as well as of sustainable water resource utilization and development, is on how to precisely evaluate the advantages and disadvantages of RW replenishment for basin health, logically plan the

allocation structure of RW, and address the issues raised by RW replenishment (Hoang at al., 2025).

RW describes sewage or wastewater that has been treated and purified to satisfy certain water quality requirements, allowing it to be safely used again in non-potable uses such industry, agriculture, and ecological water replenishment (Wigginton, 2016). Different water quality requirements apply to different reuse uses. For example: Water supply is concerned with pathogenic microbes, transparency, and water quality. Temperature, suspended solids (SS), and conductivity are given priority in industrial application. Pesticide and antibiotic residues are an issue with landscape irrigation. Water quality and quantity are important for ecological reasons. Irrigation in agriculture aims to increase the amount of phosphorus (P) and nitrogen (N). Reusing groundwater keeps an eye on the mineral concentration and salinity (Zhao et al., 2022). These requirements also rely on the source water's properties and the treatment methods used at the wastewater treatment facility. Deng et al (2019) found most established wastewater treatment plants cannot ensure to dislodge certain contaminants completely from origin water，such as seasons and influent variations, influence occurrence and concentration of reclaimed waterborne contaminants. Although the ecology impacts of reclaimed water recharge on the rivers are still unknown, especially for the microbial assemble and species coexistence in different seasons，temperature, dissolved oxygen, and ammonia nitrogen were the main driving forces（Wang et al.,2022） Numerous irreversible changes in water quality, quantity, flow patterns, ecology, and surface-groundwater exchange have been observed in water bodies that have been subjected to long-term artificial intervention by reclaimed water replenishment, according to studies. An et al (2023) found that reclaimed water use has improved water quality of domestic polluted urban rivers and increased bacterial genus level abundance. Algal bloom control in rivers replenished by reclaimed water has drawn attentions (Lv et al., 2020). Fustigation accounting for reclaimed water nutrients can substantially save fertilizers costs while

agronomical risks (Maestre-Valero, J. F et al., 2019). The reuse of reclaimed water may have enhanced the N-cycling functions of microbial communities and the emission of nitrous oxide（Alcaide Zaragoza, C et al.,2022）.but until now, reclamation treatment on wastewater does not completely remove all pollutants in water（Wang et al.,2024）.

The majority of research on RW focuses on examining changes in certain compounds in receiving soils and waters, offering qualitative evaluations of the extent of their effects (Expósito et al., 2024, Garcia-Cuerva, L et al., 2016). As an alternative, they assess the potential and hazards of using reclaimed water by looking at the physicochemical characteristics and growth circumstances of certain application targets, such as crops and plants (He et al., 2021). Yet, little is known about how water bodies—especially at the integrated basin environmental level—react to replenished water, including the relationships and patterns between different components and how to mitigate these negative impacts on basin environments and ethics (Hambly et al.,2010). Our research uses four years of extensive in-situ monitoring of the RHJ basin in Harbin, a typical water-scarce city in Northeast China, as a case study to reveal the environmental evolution patterns and response mechanisms of various environmental factors after RW replenishment. In addition to statistically evaluating the basin's hydrology, water resources, environment, and ecology, it investigates the relationships between these changes. With major scientific value and practical implications for preserving the ecological health of the studied basin and improving the quality of water resource utilization, this supports planning and decision-making for the scientific layout, optimal allocation, and sensible use of RW.

In order to accomplish these goals, our research mainly investigated three areas:

(1) Long-term, extensive, in-situ monitoring of environmental factors throughout the basin;

(2) Analysis of species ecological, hydrogeological, and soil-water

environmental evolution under conditions of RW replenishment;

(3) Exposing patterns of basin environmental change from the perspectives of water resources, water quality and hydrodynamics.

(4) Proposing management optimization strategies or RW layout that address both positive and negative environmental feedbacks within the basin.

2. Material and methods

2.1 Study area

RHJ basin (126°34′~126°41′E, 45°32′~45°45′N) is located in the central part of Harbin city. Which is originating in the southern Pingfang District and eventually empties into the Songhua River after flowing north through Daoli District **(Fig.1.**). With a basin area of 126km² and channel length of 32.59km, this naturally occurring stream was created by rainfall. The mainstream, east stream and West stream are its three portions. The semi-humid continental monsoon climate is typified by short, wet summers, with June through September seeing 60% to 80% of the year's precipitation. The average temperature throughout the long and frigid winters is -19.7°C. The river freezes over between November and April, with an average ice thickness of 0.5~1.2 meters and frozen soil depth of 0.2 meters. Along its river, the system integrates seven RW outfall points: two from Songhua River raw water, one from backwash water, and four from city sewage treatment plant effluent. The daily total inflow capacity peaks at 5.18×10^4t.

2.2 Data collection

We carried up a four-year monitoring program that covered hydrology and hydrodynamics, topography and geology, water quality, sediment and microorganisms in order to fully comprehend environmental changes in the RHJ basin after the implementation of RW replenishment.

2.2.1 Hydrology and hydrological data

The 12-month period from March 2023 to February 2024 was used for hydrological observations. Measurements were made between 9:00 AM and

4:00 PM, with an observation frequency of 15 days per cycle. Four monitoring stations were used to gather data on an hourly basis. Each station shows the discharge, flow rate, and water level at the specific river cross-section. At certain locations, objective variables such as outfall construction and ice cover resulted in data gaps. During periods of intense rainfall or flood flow, sampling was delayed until after the hydrological conditions had calmed. Slanted gauges with an error tolerance of ≤1 cm were employed to measure the water level. Leveling milestones and benchmarks were based on the Dadingzishan Hub Station downstream on the Songhua River's Harbin section. Flowmeter is used to monitor flow velocity (**Sontek FlowTracker2, Xylem.，US**). The device is suspended 0.9 meters below the water's surface by a support rod. When there is little to no ice cover, measurements can be made by carving through the ice, making that the rotating parts stay at least 0.5 meters clear of the ice. There is a 2% measuring error. To make sure there is no backflow along the vertical lines, the three-point approach is used at each cross-section using three vertical lines. The following formula can be used to determine flow rate:

$$V_m = \frac{1}{3}(V_{0.2} + V_{0.6} + V_{0.8}) \quad (1)$$

Where V_m refers vertical average flow velocity (m/s). $V_{0.2}$、$V_{0.6}$、$V_{0.8}$ refer flow velocity (m/s) at measurement points at relative water depths of 0.2, 0.6, and 0.8 m.

2.2.2 Topography and cross-sectional data

October 2021, May 2022, April 2023, and March 2024 are the survey periods. The whole RHJ basin is included in the scope, which also includes strip surveys of the land and water. The terrestrial survey covers an area of 3.6km² and stretches 50 meters outward from the crest line of the embankments on either side of the river channel. The 2000 National Geodetic Coordinate System was used as the geographic coordinate system, and the control points in the Harbin portion were derived from internal control points from the Songhua River embankment project. The National Elevation Datum of 1985 served as the

basis for elevation measurements. The accuracy parameter was mean error, and the maximum allowable error was twice the mean error. Plane control network with a projected length deformation of ≤25 mm/km was created mainly for field surveys. 1:500 scale and an error tolerance of ≤0.15m were used for the survey. For bathymetric points, the planar error ≤2mm. A single mileage system was used to number the river channel when the survey was finished. Three river segments, each one kilometer in length, were marked as A~CK+000. Four places were included in the survey cross-sections, which ran from north to south: AK0+820, BK2+100, BK12+700 and CK6+660. RTK technology (**CTI X16, Shanghai Huace Navigation Technology Ltd., DJI Mavic 3E, Dajiang Innovation., China**) was used for land surveying, while an unmanned survey vessel (**CTI 4pro, Shanghai Huace Navigation Technology Ltd., China**) was used for water surveying.

2.2.3 Water quality data

Sampling frequency of once every seven days was used for the 12-month water quality-monitoring project, which ran from March 2023 to February 2024. Three replicate collections were set up at each of the four sampling locations. At certain monitoring stations, there were data gaps because to objective variables including ice cover and construction at discharge points. When precipitation occurred during sampling periods, sampling was delayed until the rain stopped and the river conditions stabilized. A cylinder-style water sampler (**LB-8001D, Juchuang Group Co., Ltd,China**) was used to gather water samples. Before being used at each sampling location, each sampler was carefully cleaned with river water to avoid cross-contamination. After being collected, the samples were promptly taken to the laboratory (**Heilongjiang University,haerbin,China**) and stored in high-density polyethylene bottles. Prior to analysis, samples were sealed and kept below 4°C, and all analyses were finished in ten days. China's Ministry of Ecology and Environment's water quality standards were met by all analytical techniques：TN using the alkaline potassium persulfate digestion-UV spectrophotometric method; TP was

evaluated using the ammonium moly date spectrophotometric method; COD was ascertained using the potassium dichromate rapid digestion spectrophotometric method; and NH_3-N was measured using the Nessler's reagent spectrophotometric method. BOD_5 was measured. the dilution and inoculation procedure. All tests had a relative error of ≤±10%.

2.2.4 Sediment data

In June 2024, when sediment morphology and characteristics are most noticeable, sediment sampling was carried out. Four sampling locations were set up in line with water quality monitoring facilities. The water surface was accessed using a small dredging vessel that was supplied by the water conservation department. Using piston-type columnar sediment samplers that were introduced into the riverbed silt layer, manual sampling was carried out. Five sample tubes were deployed, each measuring one meter in length and four centimeters in diameter. In order to assemble the proper number of sampling tubes, the silt depth was first measured using a 3-meter polyethylene probe. After inserting the tubes into the solidified layer, a rotary cutting technique was used to cut each sediment layer into the sampler at the same time. After that, the sediment column was sealed and removed, preventing the cylinder samplers' frictional disruption of the sediment stratification. Following collection, the samples were promptly delivered in stratified, sealed containers to the laboratory (**Spectrum Company,haerbin , China**). After separating the sediment from the water, the sediment was moved to a drying chamber. Samples were sealed and kept below 4°C until they were examined for organic materials within 7 days. To determine internal phases, sediment from the QL discharge site was chosen, dried, powdered, and then exposed to X-ray diffraction examination (XRD). Every analytical technique complies with the Chinese Ministry of Ecology and Environment's Soil Monitoring Technical Specifications. The sulfuric acid-potassium dichromate oxidation-external heating method was used to measure the amount of organic matter (OM) in sediments. The semi-micro Kjeldahl digestion method was used to analyze

nitrogen (N). Using a potassium chloride solution, ammonia nitrogen (NH_3-N) was extracted and quantified using spectrophotometry. Using sodium bicarbonate, phosphorus (P) was extracted, and the molybdenum-antimony reagent was used for spectrophotometric measurement. The following heavy metals were identified: Hg by cold atomic absorption spectroscopy (CAAS), Zn and Cr by flame atomic absorption spectroscopy (FAAS), Cu and Ni by inductively coupled plasma mass spectrometry (ICP-MS), Pb by graphite furnace atomic absorption spectroscopy (AFAS), Se by X-ray fluorescence spectroscopy (XRF), Cd by graphite furnace atomic absorption spectroscopy (AFAS). ALL the above relative deviation ranged from 25~30%.

2.2.5 Microbial data

In June 2024, microbial sampling was also carried out at the discharge site and 50 meters upstream and downstream of the OF1 wastewater treatment plant. Using 16S rDNA analysis, which will be contracted out to the Heilongjiang University, microbial species identification will be carried out. The process consists of purifying bacterial DNA, amplifying the 16S sequence, purifying the amplification product, PCR sequencing, purifying the product, and machine sequencing. The samples' species categorization will be ascertained by comparing the results with the NCBI database.

2.3 Analytical methods

2.3.1 Statistical analysis

To determine the reaction patterns of environmental elements in the basin influenced by RW discharge sites, perform feature analysis of hydrological, water quality, topographical, and sediment data under various temporal, geographical, seasonal, and operational situations. To investigate the correlations between variables, correlation analysis was used. The product of the two matrices' standard deviations using Pearson's correlation coefficient divided the covariance matrix. Values near 0 signify no direct association between the two, whereas positive values indicate positive correlation and negative values indicate negative correlation. This technique calculates the

degree of association between sediments at the discharge point for RW and contaminants in the effluent. The relationship between microbial community diversity and water quality at the RW discharge point was evaluated using the Mantel test. When there is a positive correlation, the distance between samples in one matrix rises in tandem with the corresponding distance in the other matrix. A smaller p-value in the Mantel test indicates a larger correlation, suggesting that environmental influences have a greater impact on microbial populations. To examine how two objective factors—the location of discharge stations and seasonal variations—affect water quality, PCA plots were examined separately. The Kaiser-Meyer-Olkin (KMO) test and Bartlett's sphericity test were among the preliminary tests used to determine whether the water quality dataset was suitable for PCA before the PCA diagram was plotted. The success of PCA in reducing the dimensionality of the dataset was confirmed by LM's KMO value of 0.90 and the Bartlett test result of $p < 0.001$. PCA's great applicability for the majority of variables in the RHJ basin was demonstrated by the sampling sufficiency (MSA) values for water quality variables approaching one. Hydrodynamic, sediment transport, and water quality simulations were conducted using the DHI MIKE21 model's HD, SD, and ECO Lab modules. All simulation baseline data were derived from field measurements obtained during this study.

2.3.2 Analysis of microbial diversity

Our research uses microbial diversity and abundance to show how the discharge of RW affects the basin's biological systems.

1. Richness Indices

The Chao1 index estimates the true total number of species (or OTUs/ASVs) in a sample. A higher Chao1 index indicates that the sample may contain more undetected rare species, suggesting greater species richness, while a lower index indicates the opposite.

$$R_{\text{chao1}} = \text{Obs} + \frac{n_1(n_1-1)}{2(n_2+1)} \quad (2)$$

Where Ob_s refers to the number of OTUs/ASVs actually observed,n_1，n_2，n_3 refer to number of OTUs occurring only once, twice and three times.

With a focus on assessing uncommon species, the ACE index is used to determine the true species richness within a community. It works particularly well with data from 16s rRNA sequencing. Greater species richness in the community is indicated by a higher ACE score, which raises the possibility of an abundance of uncommon species that may not have been fully identified.

$$R_{\mathrm{ACE}} = 1 - \frac{F_1}{N_{rare}} \tag{3}$$

Where F_1 refers to number of singletons (species with abundance ≤1). N_{rare} Total number of individuals of rare species (the sum of all species with abundance ≤10).

2. Diversity Indices

The Shannon–Wiener index is one of the most commonly used α-diversity measures in ecology, simultaneously accounting for species richness and species evenness. Higher values indicate greater diversity.

$$D_{Shannon} = -\sum_{i=1}^{S} p_i \ln p_i \tag{4}$$

Where S refers to number of species actually observed. P_i refers to Relative abundance of the i-th species, where:

$$p_i = \frac{n_i}{N} \tag{5}$$

Where n_i refers to the number of individuals of the i-th species. N refers to total number of individuals across all species.

The likelihood that two randomly chosen members of a community are members of the same species is measured by the Simpson index. Diversity is higher when the likelihood is lower and lower when the probability is higher.

$$D_{simpson} = \sum_{i=1}^{S} P_i^2 \tag{6}$$

Where Pi=n·i/N，S refers to number of species.

2.3.3 Plotting processing

The topographic analysis map was made with ArcGIS 10.8. Resources from Tianditu (the National Geographic Information Public Service Platform) are used in the imagery map. Hydrodynamic simulations were conducted using

MIKE21 software from DHI.The ggplot package in R Studio 4.3.2, Origin 2021, GraphPad Prism 10.1.2 and Photoshop 2021 was used to create all additional figures and charts.

3. Results

3.1 Evolution of hydro-topographic conditions

3.1.1 Hydrological parameters

We conducted monthly monitoring of flow velocity, discharge, and water level at the river section receiving effluent from four wastewater treatment plants (OF1~OF4) from March 2024 to February 2025（**Fig.2.**）. As the dominant discharge source (2.5×10^4 t/d), OF1 exhibited pronounced seasonal variability, with peak flow velocities averaging 5.31 m/s (maximum 6.10 m/s) in September 2024, representing a 71.3% increase compared to December baseline measurements (3.10 m/s). Comparative analysis revealed that while OF1's July velocity (3.84 m/s) approximated that of OF2 (2.01 m/s), its mean discharge rate (0.08 m^3/s) constituted only 12.3% of OF2's capacity (0.65 m^3/s) due to constrained cross-sectional dimensions.

The western stream exhibited OF1-dominated hydrology, with average August velocities of 4.56 m/s (peak 5.27 m/s) and a discharge rate of 1.15 m^3/s, confirming the anticipated positive correlation ($r = 0.89$, $p < 0.01$) between flow velocity and cross-sectional area. Seasonal contrasts were evident, with summer (July–September) discharge rates (0.88 m^3/s) exceeding winter (December–February) averages by 27.5%. Water level dynamics showed that OF1's long-term average (154.2 m; maximum 154.6 m) significantly surpassed those of other outlets (OF3: 133.9 m; OF4: 148.9 m), with autumn base flow reductions causing marginal declines (154.5 m in March vs. 154.4 m in October, $\Delta = 0.07\%$), mitigated by recycled water replenishment strategies (Cheng et al., 2021).

The eastern stream (OF4 discharge zone) experienced pronounced flow intermittency, with zero-flow conditions persisting from January to April 2024,

contrasting with flood-season maxima of 0.33 m/s velocity and 0.79 m^3/s discharge. OF3 displayed phased discharge fluctuations (September: 0.26 m^3/s; November: 0.35 m^3/s, +34.6%). Statistical modeling revealed strong wet-season interdependence among hydrological parameters at OF2 (velocity-discharge $r = 0.92$, $p < 0.01$; level-discharge $r = 0.87$, $p < 0.01$), whereas dry-season correlations diminished to 0.58–0.61, indicating altered baseflow regimes under water suspension conditions (Kampf et al., 2016). Cumulative analysis confirmed that OF1-OF2 contributed over 70% of total summer discharge, while low-flow outlets (OF4) demonstrated heightened sensitivity to operational constraints.

3.1.2 Topographic Elevation

Long-term topographic evolution analysis (2021–2024) revealed distinct geomorphological changes along the upstream downstream transects of four discharge points (**Fig 3**). At OF2, persistent elevation differentials were observed: upstream elevations were 131.31 m (+0.19 m) in 2021, 130.00 m (–0.20 m) in 2022, and 130.40 m (+0.18 m) in 2023, relative to downstream sections. Barometric data confirmed a gradual downstream aggradation trend, with elevation advantages stabilizing at ≈0.5 m by 2024, indicative of sustained sediment deposition from effluent transport. Parallel measurements at OF2 demonstrated upstream dominance (116.64 m, +0.34 m in 2021; 114.52 m, +0.42 m in 2024), while downstream sections showed progressive elevation increases through sediment accretion. The OF1-controlled estuarine zone exhibited characteristic channel width variations (wide-narrow-wide configuration), shaped by urban infrastructure constraints. High-resolution bathymetry revealed a prominent left-bank sandbar formation, with concomitant constriction of the main channel to a 30 m width. This geomorphic adjustment induced preferential sediment accumulation in low-velocity zones (left bank: +0.3 m/yr. deposition rate), consistent with secondary flow dynamics described by Simmons et al. (1989). Basin-scale analysis confirmed discharge-driven elevation modifications through coupled erosion-deposition processes

(Pradhan et al., 2021): localized aggradation (+0.1–0.5m) alternated with erosional zones (–0.05–0.15m), especially during the 2022 dredging interventions. Post-dredging monitoring (2023) documented sediment recovery rates of 0.08–0.12 m/yr, validating the system's resilient sediment equilibrium (Pontee et al., 2004).

3.2 Spatial and temporal variations in water quality

Comprehensive analysis of wastewater effluent quality (2024–2025) revealed significant inter-point variability in pollutant emissions **(Fig.4.**). OF4 exhibited the highest COD loadings, with peak concentrations exceeding 60 mg/L (annual mean: 45±3.2mg/L) and high-value anomalies occurring in 15% of measurements, indicative of intermittent organic pollution shocks. In contrast, OF3 exhibited the lowest COD levels (22±1.8mg/L), reflecting superior pretreatment efficacy. Nitrogen pollution exhibited distinct spatial patterns: OF1 discharges contained elevated NH_3-N (peak 4.2 mg/L, fluctuations >3 mg/L) and TN concentrations (maximum >5 mg/L, double OF3's 1.8 mg/L), confirming its dominance in nitrogen emissions. Phosphorus distribution followed a gradient, with OF1–OF2 means (0.35–0.3 mg/L) exceeding that of OF3 (0.2 mg/L), while OF4 exhibited episodic TP spikes (>0.5mg/L).BOD_5 monitoring identified OF4 as the primary source of biodegradable organic matter (annual mean: 6 mg/L, 12% anomaly frequency). Strong COD-BOD_5 covariation ($r=0.85$, $p < 0.001$) (Rhew et al., 2016) confirmed consistent organic matter inputs, whereas weak TP–N correlations ($r<0.4$) suggested divergent nutrient pathways. COD-TN/NH_3-N moderate correlations ($r=0.6–0.7$) aligned with domestic wastewater characteristics (Hao et al., 2022). Inter-point comparisons revealed similarity between OF1 and OF2 (COD, $r = 0.68$) and disparity between OF4 and OF3 ($r=0.32$), reflecting treatment process heterogeneity (Nancharaiah et al., 2023). These findings collectively identify OF1 and OF4 as priority control points for nitrogen and organic pollution, respectively, while highlighting the need for phosphorus-specific management strategies.

3.3 Sediment properties and contamination

Stratified sediment sampling (0.2m intervals) revealed distinct contamination profiles across discharge points（Table 1）, with OF3 exhibiting exceptional organic enrichment (P4-L2 layer: OM = 5630 mg/kg, N = 4770 mg/kg), 22.4–110% higher than other sites (OF1: 4600 mg/kg; OF2: 2680 mg/kg; OF4: 3460 mg/kg). Heavy metal distribution exhibited point-source characteristics: Zn peaked at 516 mg/kg in OF2's P3-L3 layer, consistent with historical metalworking effluent (Rakesh et al., 2021), while OF3 showed elevated Cr (78 mg/kg) and Cd (0.74 mg/kg) in surface layers, attributable to legacy industrial land use (Juhasz et al., 2011). XRD analysis of OF1 sediments identified dominant (Na,Ca)Al $(Si,Al)_3O_8$ (5000 a.u.) and $C_4H_8N_2O_2$ (5300 a.u.) phases**(Fig.5.**), confirming nitrogenous organic accumulation through anaerobic fermentation (Sharma et al., 2013). ICP quantification detected prevalent flocculent-derived metals (Al: 36.13 mg/g; Fe: 49.76 mg/g), constituting 94.3% of measured heavy metals, a signature of wastewater treatment residuals (Shrestha et al., 2020). These findings systematically characterize the sedimentation dynamics of effluent-derived contaminants, identifying OF3 as the critical organic/nutrient sink and OF2 as the primary zinc repository in the basin.

3.4 Microbial community characterization

Longitudinal analysis of sediment microbial communities along the OF1 discharge gradient revealed distinct spatial stratification (Table 2). α-Diversity metrics showed maximal values at the immediate discharge point (Chao1 = 3124, ACE = 3182.58, Shannon = 6.23), exceeding those at both upstream (Chao1: 2396, ACE: 2578.60, Shannon: 5.61) and downstream (Chao1: 2626, ACE: 2653.57, Shannon: 6.51) stations. OTU distribution patterns (downstream: 3124 > discharge point: 2626 > upstream: 2035) indicate wastewater-mediated enrichment, with peak microbial richness at the discharge interface and maximal population density in downstream transport zones. Community composition shifts exhibited wastewater-selected succession: Proteobacteria

and Bacteroidetes collectively increased from 38.7% upstream to 67.2% at the discharge point and 71.5% downstream, characteristic of organic-rich wastewater adaptation (Anna et al., 2019). Downstream sediments specialized in Gammaproteobacteria (18.3% vs. 9.7% upstream), while discharge point samples were enriched in Bacteroidetes (29.4%). Upstream communities maintained Actinobacterial dominance (41.2%), reflecting pristine sediment conditions (Bian et al., 2025).This tripartite zonation (**Fig. 6**) demonstrates: (1) acute wastewater selection at discharge points (abundance peak), (2) community restructuring during transport (diversity maximization), and (3) establishment of pollution-dependent ecological gradients, corroborating the pollutant-microbial feedback mechanism proposed in our sediment chemistry analysis (R^2 = 0.83 between COD and Proteobacteria abundance).

4. Discussion

4.1 Improvement of water resources supply and allocation

Given variations in water replenishment conditions across different sections of the RHJ basin, we divided the basin into eight segments based on major discharge points and weir locations, assigning each segment a station number (**Fig.7.(b)**). Before water replenishment, we calculated the channel storage capacity using rainfall intensity, catchment area, runoff coefficient, and surface type. After replenishment, we recalculated and analyzed water resource quantities under both conditions. Under water replenishment conditions, total water resources in the main stem increased from approximately 2.5×10^4~3×10^4 m^3, representing a growth of about 20%. This increase primarily resulted from the convergence of two upstream tributaries. The eastern and western branches exhibited particularly significant growth (**Fig.7.(a)**): the eastern branch increased from 1.0×10^5~$1.8\times10^5 m^3$ (approximately 80%), with a single water replenishment point (OF4) at its headwaters directly determining its total water resources. The West Branch increased from 1.5×10^5~$2.0\times10^5 m^3$, a 33% increase. As the longest channel,

the West stream relies solely on replenishment from the OF2 and OF3 outlets to maintain its base water level. These figures indicate that, before water replenishment, the water volume relied solely on natural precipitation and storm water inflows. As analyzed in Section 3.1.1 regarding hydrological parameters, discontinuing replenishment in east stream, for instance, would cause significant drying in downstream sections—particularly at northern locations—where seasonal drought is the primary constraint (Pei et al.,2023). Segmented water replenishment significantly improved water resource distribution within the basin, with the most pronounced effects observed in the East and West stream sections. Except during the ice-bound season, channel flows were maintained between 2~3 m^3/s. Consequently, water replenishment plays a positive role in basin water resource recovery and ensuring ecological flow (Virkki et al., 2021)

4.2 Evaluation and analysis of the quality of the water and sediment

4.2.1 Spatial and Temporal Variations in Water Quality

Quantitative analysis from the spatial differentiation and seasonal dynamics dimensions revealed the variation patterns and driving mechanisms of water quality and sediment pollution in the RHJ basin. At the spatial scale（**Fig.8.(a)**）, the first principal component (PCA1) explained 53.68% of the variance, while the second principal component (PCA2) explained 20.97%. Together, they accounted for 74.65% of the variance. Indicators such as sediment organic matter (OM (SD)), biochemical oxygen demand (BOD), and chemical oxygen demand (COD) showed high positive loadings on PCA1, while ammonia nitrogen (NH_3-N) exhibited negative loadings. Total nitrogen (TN), sediment nitrogen (N (SD)), and total phosphorus (TP) also exhibited positive loadings on PCA1. Samples from the four discharge points (OF1-OF4) showed significant clustering heterogeneity, with OF2 samples strongly correlated with organic pollution indicators and OF4 samples strongly correlated with nitrogen and phosphorus indicators. Univariate ANOVA revealed highly significant effects of discharge points on PCA1 scores ($F=18.52$, $p<0.01$). Multiple

comparisons (Tukey's HSD) revealed highly significant differences in PCA1 scores between OF2 and OF4 ($p=0.005$) and between OF2 and OF1 ($p=0.015$). Combined with the water quality analysis in Section 3.2, this suggests that discharge characteristics vary across different outfall locations due to differences in effluent indicators. At the seasonal scale (**Figure.9.(b))**, for the OF1 discharge point), PCA1 explained 49.33% and PCA2 explained 28.07% of the variance, cumulatively accounting for 77.4% of the total variance. Spring samples were strongly correlated with NH_3-N, suspended solids (SS), and COD; summer samples were closely linked to TP and electrical conductivity (EC); autumn samples exhibited strong associations with dissolved oxygen (DO), BOD_5,and organic matter (OM(SD)); winter samples showed significant correlations with sediment nitrogen (NH_3-N(SD), N(SD)) and transparency. Univariate ANOVA revealed a highly significant effect of season on PCA1 scores ($F=23.76$, $p<0.01$). The mean scores across groups were spring 1.24, summer 0.87, autumn 1.12, and winter 0.75. Post-hoc comparisons showed significant differences between spring and summer ($p = 0.012$), and between spring and autumn ($p=0.008$). Season significantly influenced PCA2 scores ($F=12.43$, $p<0.05$), with inter-group means of: spring 0.92, summer 0.15, autumn 0.83, and winter 0.80. Multiple comparisons revealed significant differences between spring and autumn ($p =0.035$), and between winter and autumn ($p=0.042$). Spring snowmelt runoff pollution inputs caused a short-term deterioration in water quality (Miller et al., 2020, Sharma et al., 2013). Enhanced biological activity in summer and autumn degraded and consumed organic pollutants (Collins et al., 2019). By winter, low temperatures inhibited microbial decomposition, leading to nitrogen retention in the sediments. These seasonal hydrological-biological processes significantly regulated pollutant composition and the "sediment-water quality" interaction. The PCA analysis of these primary spatial and temporal factors provides a mechanistic basis and quantitative evidence for spatially precise pollution tracing and seasonally differentiated management under the influence of basin discharge.

4.2.2 Sediment-water interaction behavior

Through correlation heat maps and cluster analysis（**Fig.9**.）, with the OF1 as the monitoring section, this study reveals the correlation patterns and underlying mechanisms of multiple indicators within the "water-sediment" system of the downstream river channel. Water quality organic pollution indicators (COD, BOD_5) showed strong positive correlations with sediment Cu and NH_4-N (0.68**, 0.62**, $p < 0.01$). This core cause arises from the fact that the OF1 discharge point is the outfall of Harbin's Qunli Wastewater Treatment Plant, which primarily treats domestic sewage from the old city district. Organic matter (COD, BOD_5) and ammonia nitrogen in domestic sewage are simultaneously discharged. The presence of Cu is attributed to corrosion in most pipelines in the old city district, which were constructed in the last century and are now deteriorating due to a lack of maintenance. pH showed strong negative correlations with As (-0.69**) and organic matter (OM) (-0.52*, $p <0.05$). On the one hand, acidic conditions enhance arsenic's chemical reactivity, promoting its dissolution from sediments into the water body. On the other hand, microbial decomposition of sedimentary OM produces acidic metabolic byproducts that counteractively regulate water pH, forming a "pH-OM-As" interactive chain. Transparency negatively correlates with Ni (-0.55*), as Ni enrichment promotes sediment particle aggregation and suspension, increasing turbidity and reducing light penetration—demonstrating the indirect impact of heavy metals on water physical properties. Turbidity positively correlates with TP (0.38*) and COD (0.42*), as suspended particles adsorb and complex phosphorus and organic pollutants through their large surface area and active sites. Hydro dynamically driven particle migration constitutes the key pathway for "water-sediment" exchange (Carhart at al., 2024). Positive correlations exist between Pb and Cd (0.58**), and Zn and Cr (0.50*), reflecting decades of cumulative impacts from electroplating and metallurgical industries in Northeast China's old industrial bases on urban water and soil environments. Due to the co-discharge characteristics of industrial wastewater containing

multiple metals, these heavy metals accumulate synergistically in sediments through transfer between surface and groundwater. The correlation analysis between sediments and water comprehensively explains, from dimensions including pollution sources, geochemical cycles, and interfacial physicochemical interactions, how the quality of effluent discharged from outlets affects sediment properties in receiving water(Emily at al.,2018), thereby influencing water quality changes. This demonstrates the significant influence of discharge outlets on river environment.

4.2.3 Impact of outfall water quality on microorganisms

Using Mantel tests and cluster analysis（**Fig.10.**）, with the OF1 as the sampling point, we conducted an in-depth analysis of the interactive relationships between downstream water quality and microbial richness, diversity, and evenness indices. The cluster tree clearly divides microbial indicators into three major groups: abundance, diversity, and evenness. In the Mantel test, edge width corresponds to Mantel's r (indicating the strength of the distance correlation), while edge color reflects statistical significance based on 9999 permutations. Pearson correlation analysis revealed that the abundance index showed a significant positive correlation with electrical conductivity (EC) ($r = 0.42$, $p < 0.01$) and total phosphorus (TP) ($r = 0.38$, $0.001 < p < 0.01$), and a significant negative correlation with transparency ($r = -0.35$, $0.01 < p \leq 0.05$). This is because EC, representing ionic strength, and TP, which provides phosphorus sources, establish the material foundation for microbial proliferation. Conversely, reduced transparency leads to increased turbidity, which inhibits light-driven microbial metabolism, consequently affecting abundance. Diversity indices showed a significant positive correlation with chemical oxygen demand (COD, $r = 0.35$, $p < 0.01$), biochemical oxygen demand (BOD_5) ($r = 0.30$, $0.01 < p \leq 0.05$), and a significant negative correlation with ammonia nitrogen (NH_3-N) ($r = -0.32$, $0.01 < p \leq 0.05$). This stems from the organic substrates carried by COD and BOD_5, which provide energy for microbial community succession, while the bio toxicity of high NH_3-N

concentrations inhibits group diversity. However, excessive NH_3-N concentrations induce bioaccumulation of toxins, which suppress species diversity. The evenness index showed a significant positive correlation with EC ($r = 0.39$, $p < 0.01$) and TP ($r = 0.36$, $0.001 < p \leq 0.01$), and a significant negative correlation with turbidity ($r = -0.33$, $0.01 < p \leq 0.05$). Gradient changes in EC and TP promote differentiation at the phylum and genus levels, facilitating uniform microbial distribution. Increased turbidity intensifies resource competition among populations within the same category, thereby reducing community evenness. Quantifying these multidimensional relationships reveals how water environmental factors, such as ionic strength, nutrient salts, and organic load, regulate microbial community structure (Zhang et al., 2022). This explains how prolonged drainage alters microbial community characteristics in both sediments and water bodies within river channels (Lu et al., 2022), ultimately determining long-term population succession.

4.3 Effect and variation in hydrodynamic conditions

Based on the HD, ST, and ECO Lab modules within the MIKE21 model, the operational scenario was established with four wastewater treatment plant outfalls along the entire river receiving regular replenishment. The open and closed boundaries were defined as the headwaters of the East and West stream, and the river mouth, respectively. Point source discharges were added incrementally based on station numbers. Using the measured hydrological, water quality, and sediment data from Section 2.2, this study revealed variations in hydrology, hydrodynamics, sediment transport, and water quality across different segments of the recharge-type basin. Regarding flow rate (**Figure 11(a)**), the main channel segment (AK0+000~AK3+100) exhibited flow velocities of 4.5~6m³/s, while the West Branch section (AK3+100~CK6+630) exhibited a decrease to 3.5~4.5m³/s. The East Branch section (BK2+500~BK21+919) further reduced to 2.5~3.5m³/s, showing a gradient decrease along the tributary branches. This is primarily due to differing discharge volumes at each wastewater treatment plant outlet: the main

channel's OF1 contributes 250,000 t/d, while the eastern stream headwaters provide only 20,000 t/d. Although the peak replenishment flow of the western stream reaches 24.8 t/d, winter conditions significantly constrain its flow rate due to weather and operational limitations. Moreover, the western stream's total length of approximately 22km causes high flow rates to decrease during transit. Regarding flow velocity (**Figure 11(b)**), the overall pattern mirrors that of flow rate: the main channel segment exhibits velocities of 1.5~2.5m/s, the western tributary segment exhibits 1.0~1.5m/s and the eastern tributary segment exhibits 0.5~1.0m/s. This is primarily due to the relatively narrow main channel with concentrated inflow, which results in stronger hydrodynamics. This primarily reflects variations in the channel's cross-section. The main channel segment is the narrowest in the entire basin and incorporates a spillway gate, causing significantly higher velocities for upstream converging flows at this point. However, at the estuary segment, channel constriction and changes in configuration create a slow-flow zone upstream of the river mouth. Scour and fill depths **(Figure 11(c)**) closely correlate with hydrodynamics: the main channel section exhibits scour and fill depths of 1.5~2m, consistent with the topographic simulation analysis in Section 3.1.2. The west section shows 0.2~0.5m, while the east section shows 1.0~1.5m. stronger hydrodynamics promote deeper sediment scour. The short length and high velocity of the main stem section, along with high flow volume, result in the highest scouring rates and depths. Although the eastern channel receives less replenishment flow, its bed is inherently higher and is primarily subjected to scouring from runoff along both banks (Shen et al., 2024). Water quality analysis using NH_3-N as an indicator (**Figure 11(d)**) shows NH_3-N concentrations of 2~3mg/L in the main channel section, while the western tributary section recorded 3~4.5mg/L, and the eastern tributary section recorded 4.5~6mg/L. The increasing NH_3-N concentration in the middle and lower reaches correlates with pollutant accumulation from discharge points carried downstream and a reduced hydrodynamic dispersion capacity due to decreased flow velocity. Collectively,

these results demonstrate that hydrological changes induced by discharge points within the basin significantly influence sediment transport and the evolution of water quality (Wang et al., 2025).

4.4 Strategies for addressing water environment issues in river basin and recommended management solutions

RHJ basin, a vital water system in Harbin's urban core, serves dual functions of flood drainage and landscape enhancement. Many urban waterways in Northeast China experience seasonal drying, water scarcity, severe pollution, and siltation. This study conducted comprehensive experiments and analyses encompassing hydrology, topography, water quality, and ecology. It revealed that, despite engineering measures for RW replenishment, these interventions significantly influence the basin's ecological environment from a sustainable development perspective. To mitigate the adverse effects of discharge points and gradually allow the basin to adapt more naturally to this model, fostering a stable and healthy aquatic environment, we propose segmented and categorized environmental restoration strategies for the RHJ basin based on the findings of this study **(Fig.12.)**. Managers and decision-makers offer these strategies for reference.

1. Upgrading wastewater treatment plants: Improve treatment standards at wastewater treatment plants along the route, upgrading from Class I to Surface Water Category V, reducing pollution at the source.

2. Dredging and desilting Conduct annual dredging at the river mouth, confluence points, and east stream areas prone to recurring siltation—to clear blockages and reduce the release of internal pollutants.

3. Water replenishment and diversion: Utilize the wetland park along the main stream and the upper reaches of west stream to develop artificial wetlands. Divert part of the river flow and raw water from the Songhua River into these wetlands for purification before returning it to the river, thereby introducing ecological flow.

4. Storm water-sewage separation: Accelerate the separation of urban

storm water and sewage pipelines to reduce wastewater discharge into rivers.

5. Ecological bank protection: Ecologically restore natural banks along the middle and upper reaches of west stream to mitigate soil erosion from water scouring and reduce upstream sediment transport.

6. Estuary renovation: Based on the existing river morphology, clear silted sections at the estuary and construct diversion dikes. Integrate landscape design to create an estuary park.

7. Enhanced daily management: Establish a dedicated management team and a professional operating company to conduct daily patrols provide real-time feedback on basin environmental issues, and implement immediate corrective actions.

4.5 Limitations and Outlook

Due to objective constraints, hydrological, water quality, and sediment samples in this study were collected and analyzed at limited times and locations. Consequently, the conclusions are of short-term representativeness. However, to gain deeper insights into watershed environmental evolution and human interventions, we must extend data collection over a period exceeding five years.

The environmental impact of RW replenishment remains largely a black-box model. This study tentatively elucidates mechanisms through surface observations and geophysical-chemical processes; however, clarifying the true reaction mechanisms requires further interdisciplinary collaboration.

Our research may not alter the basin's water replenishment framework in practice, as this represents an extremely large-scale and costly endeavor that requires significant changes to existing conditions. We aim solely to improve and remediate the basin's environment within the current framework while providing scientific insights for planning RW systems in other similar northern basins.

5. Conclusion

In conclusion, our long-term research objectives go beyond merely analyzing hydrological, geological, and ecological data within the basin. We aim to propose optimizations for basin planning, urban development, and the scientific design of urban RW supply systems in Northeast China. Additionally, we aim to gradually adapt the basin to this artificial intervention, restoring its natural health and minimizing environmental impacts.

Hydrological Conditions and Topographical Evolution: During the summer flood season (July-August), flow velocities reach 3.1~6.1m/s, characteristic of high-flow conditions. This poses no threat to the well-constructed embankments (P = 1%) along the main channel. However, flow rates vary across cross-sections, with the widest section (OF2) showing a flow rate of 1.15 m^3/s. downstream elevations of discharge points generally exceed upstream levels by 0.5~1.0 m, especially at the river mouth. This disparity was most pronounced before the 2022 dredging, with a slight rebound after one year. Sedimentation downstream indicates a correlation between long-term discharge of SS and TP and pollutant accumulation on the riverbed. COD, NH_3-N, and BOD_5 are the primary organic pollutants in the river, originating from domestic sewage treatment plants at discharge points, contributing to the river's black and odorous condition. Organic matter in sediments decreases vertically, with the highest organic concentration at OF1 and heavy metals most concentrated at OF2, stemming from early industrial development. Microbial diversity downstream is significantly higher than upstream, resembling that in activated sludge processes at treatment plants.

After RW supplementation:

Water Resources: Total reservoir storage increased from 1.01million m^3~1.36 million m^3, a 34.62% increase. Annual flow rates remained above 2~3 m^3/s, except during freezing periods, with 70% of river sections maintaining 2 m water depth, eliminating drought conditions.

Aquatic Environment: Water replenishment points significantly influence river water quality fluctuations. Water quality is better at OF2 and OF3 compared to OF1, due to upstream effluent quality. Water quality deteriorates during summer and early spring, mainly from temperature and snowmelt runoff. Outfall water quality correlates with chemical properties and microbial diversity in downstream sediments. Model simulations show improved hydrodynamics and scour depths of 1.5~2 m in the main channel. The sedimentation rate is 0.2~0.3 m/a, with most sediments transported into the Songhua River after the flood season.

In Summary: The segmented placement of RW discharge points has ensured water resources and improved hydrodynamics in localized sections of the RHJ basin. Consequently, the basin's environment and ecology are increasingly dependent on discharge water quality. Seasonal responses show that any fluctuation in discharge quality triggers stress in the aquatic environment. Therefore, we propose strategies including wastewater treatment upgrades, dredging, water replenishment, storm-sewer separation, and soil conservation. With long-term management, this approach aims to mitigate RW impacts and create a safe, free-flowing, and stable basin. This transforms RW supplementation into a positive force for ecosystem development.

CRedit authorship contribution statement

Qiuyi Ge： Writing – review & editing, Writing – original draft, Methodology, Formal analysis, Conceptualization**. Gongjin Zhang：** Investigation, Formal analysis, Data curation. **Chengli Zhu:** Methodology, Validation, Resources. **Shiwen Zhao:** Project administration, Funding acquisition. **Xing Huang：** Formal analysis, Data curation**. Genxiang Feng:** Funding acquisition.

Data availability

Data will be made available on request.

Declaration of competing interest

The authors declare that they have no known competing financial interests or personal relationships that could have appeared to influence the work reported in this paper.

Acknowledgements

The National Natural Science Foundation of China (Grant No.52209051), Basic scientific research business of central level public welfare research institutes (Grant No. Y923015), The Technology Demonstration Project of the Ministry of Water Resources (Grant No.SF-202408).

References

A, A. C. H. , A, R. K. H. , B, M. V. S. , C, A. B. , A, R. M. S. , & A, S. J. K.2010. Fluorescence monitoring at a recycled water treatment plant and associated dual distribution system – implications for cross-connection detection. *Water Research*, 44 (18), 5323-5333.

A, A. P., B, K. K., B, D. R., & A, K. G.2019.Microbial quality of wild shellfish in a tropical estuary subject to treated effluent discharge. Environmental Research, 181.

Alcaide Zaragoza, C., Fernández García, I., Martín García, I., Camacho Poyato, E., & Rodríguez Díaz, J. A.,2022. Spatio-temporal analysis of nitrogen variations in an irrigation distribution network using reclaimed water for irrigating olive trees. *Agricultural Water Management*, 262, 107353.

An, S., Song, Y., Fu, Q., Qi, R., Wu, Z., & Ge, F., et al. 2023. Reclaimed water use improved polluted water's self-purification capacity--evidenced by water quality factors and bacterial community structure. *Journal of cleaner production*, Feb.1, 386.

B., L., Simmons, S., L., & Trengove. 1989. Impact of catchment urbanization on Lake Macquarie (Australia). *Water Science and Technology*, 21 (2), 205-210.

Bian, R., Cao, X., Peng, J., Qi, W., 2025. Impact of domestic and industrial effluent discharge on the microbiome of river sediments from the middle and lower reaches of the Yangtze River. *Environ. Res*. 285(Pt 4), 122611. https://doi.org/10.1016/j.envres.2025.122611.

Carhart, A. M., Drake, D. C., Fischer, J. R., Houser, J. N., Jankowski, K. J., & Kalas, J. E., et al. 2024. Intrinsic and extrinsic regulation of water clarity in a large, floodplain river ecosystem. *Ecosystems*, 27(3).

Cheng, D., Zhan, H., Hou, X., Guo, J., & Feng, S.,2021. The evolutional states of seasonally losing unclogged stream-groundwater systems. *Journal of Hydrology*, 603.

Collins, S. M., Yuan, S., Tan, P. N., Oliver, S. K., Lapierre, J. F., Cheruvelil, K.

S., et al.,2019. Winter precipitation and summer temperature predict lake water quality at macroscales. *Water Resources Research*, 55, 2708–2721. https://doi.org/10.1029/2018WR023088.
Craddock, H. A., Rjoub, Y., Jones, K., Lipchin, C., Sapkota, A. R., 2021. Perceptions on the use of recycled water for produce irrigation and household tasks: A comparison between Israeli and Palestinian consumers. *J. Environ. Manag*. 297, 113234. https://doi.org/10.1016/j.jenvman.2021.113234.
Deng, S., Yan, X., Zhu, Q., Liao, C., 2019. The utilization of reclaimed water: possible risks arising from waterborne contaminants. *Environ. Pollut*. 254(Pt A), 113020. https://doi.org/10.1016/j.envpol.2019.113020.
Ding, Y., Liu, X., Fu, H., 2022. The effect of recycled water information providing on public acceptance of recycled water: an eye-tracking experiment. *Resour. Conserv. Recycl*. 185, 10. https://doi.org/10.1016/j.resconrec.2022.106450
Emily, H., Anne, N., Dawit, B., Gang-Jun, L., Matthew, C., 2018. A method for separation of heavy metal sources in urban groundwater using multiple lines of evidence. Environ. Pollut., 241, 787-799. https://doi.org/10.1016/j.envpol.2018.05.025.
Expósito, A., Díaz-Cano, E., Berbel, J., 2024. The potential use of reclaimed water for irrigation purposes: Is it overestimated? *Water Resour. Manage*. 38, 4541–4554. https://doi.org/10.1007/s11269-024-03878-w
Foglia, A., González-Camejo, J., Radini, S., Sgroi, M., Li, K., Eusebi, A., et al., 2023. Transforming wastewater treatment plants into reclaimed water facilities in water-unbalanced regions: An overview of possibilities and recommendations focusing on the Italian case. *J. Clean. Prod*.
Garcia-Cuerva, L., Berglund, E. Z., Binder, A. R., 2016. Public perceptions of water shortages, conservation behaviors, and support for water reuse in the U.S. *Resour. Conserv. Recycl*. 113. 106-115. https://doi.org/10.1016/j.resconrec.2016.07.015.
He, C., Liu, Z., Wu, J., et al., 2021. Future global urban water scarcity and potential solutions. *Nat. Commun*., 12, 4667. https://doi.org/10.1038/s41467-021-25026-3.
Hoang, U., Holt, J., Mahmoud-Elhaj, D., Asif, M., Tanner, B., Feltz, A., 2025. Developing a measure of trust in recycled water. *Water Environ. J*. https://doi.org/10.1111/wej.12987.
Hou, C., Fu, H., Liu, X., Wen, Y., 2020. The effect of recycled water information disclosure on public acceptance of recycled water—evidence from residents of Xi'an, China. *Sustain. Cities Soc*. 102351. https://doi.org/10.1016/j.scs.2020.102351.
Juhasz, A. L., Weber, J., Smith, E., 2011. Impact of soil particle size and bio accessibility on children and adult lead exposure in peri-urban contaminated soils. *J. Hazard. Mater*. 186(2-3), 1870-1879. https://doi.org/10.1016/j.jhazmat.2010.12.064.
Kaiyue, H., Lishuai, Z., Yongchen, Z., Qiang, H., Mingzhe, G., 2022. The relationship analysis and reaction mechanism of carbon, nitrogen, and

phosphorus metabolism in sewage treatment in plateau habitat. *Environ. Monit. Assess*. 194(7), 1-21. https://doi.org/10.1007/s10661-022-10345-x.
Kampf, S. K., Faulconer, J., Shaw, J. R., Sutfin, N. A., Cooper, D. J., 2016. Rain and channel flow supplements to subsurface water beneath hyper-arid ephemeral stream channels. *J. Hydrol.*, 536, 524-533. https://doi.org/10.1016/j.jhydrol.2016.02.050.
Lv, X., Zhang, J., Liang, P., Zhang, X., Huang, X., 2020. Phytoplankton in an urban river replenished by reclaimed water: Features, influential factors and simulation. *Ecol. Indic.*, 112, 106090. https://doi.org/10.1016/j.ecolind.2020.106090.
Maestre-Valero, J. F., Gonzalez-Ortega, M. J., Martinez-Alvarez, V., Gallego-Elvira, B., Conesa-Jodar, F. J., Martin-Gorriz, B., 2019. Revaluing the nutrition potential of reclaimed water for irrigation in southeastern Spain. *Agric. Water Manag*. 218, 174-181. https://doi.org/10.1016/j.agwat.2019.03.017.
Miller, S. A., Lyon, S. W., Miller, S. N., 2020. Quantifying daily versus annual contributions of snowmelt water to streamflow using graphical and chemical hydrograph separation. *Hydrol. Process*. https://doi.org/10.1002/hyp.13789.
Nancharaiah, Y. V., Sarvajith, M., 2023. Granular stability, nitrogen and phosphorus removal pathways of aerobic granular sludge treating real municipal wastewater at different temperatures. *J. Environ. Chem. Eng*., 11(5). https://doi.org/10.1016/j.jece.2023.111850.
Pei, W., Hao, L., Fu, Q., Liu, H., Ren, Y., Li, T., 2024. Analysis of spring drought in Northeast China from the perspective of atmosphere, snow cover, and soil. CATENA, 236, 107715. https://doi.org/10.1016/j.catena.2023.107715.
Pontee, N. I., Whitehead, P. A., et al., 2004. The effect of freshwater flow on siltation in the Humber Estuary, North East UK. Estuar. Coast. Shelf Sci., 60(2), 241-249. https://doi.org/10.1016/j.ecss.2004.01.014.
Pradhan, C., Chembolu, V., Dutta, S., & Bharti, R., 2021. Role of effective discharge on morphological changes for a regulated macro channel river system. Geomorphology, 385, 107718.
Rhew, D., Lee, S., Jaewoong, S., Seunghyun, K., 2016. Relationships between water quality parameters in rivers and lakes: BOD5, COD, NBOPS, and TOC. *Environ. Monit. Assess*. 188(4), 252. https://doi.org/10.1007/s10661-016-5243-9.
Wang, N., Hu, H., Xiao, W., Tan, Q.-G., Chen, R., Xie, M., Simpson, S. L., 2025. Hydrodynamic perturbations on contaminant behavior in low-permeability sediments: porewater metal dynamics and risk assessment implications. *Environ. Pollut*. 377, 126466. https://doi.org/10.1016/j.envpol.2025.126466.
Lu, Q., Mao, J., Xia, H., Song, S., Chen, W., Zhao, D., 2022. Effect of wastewater treatment plant discharge on the bacterial community in a receiving river. *Ecotoxicol. Environ. Saf.* 239, 113641. https://doi.org/10.1016/j.ecoenv.2022.113641.
Shrestha, R., Ban, S., Devkota, S., Sharma, S., Joshi, R., Tiwari, A. P., Kim, H. Y., Joshi, M. K., 2021. Technological trends in heavy metals removal from

industrial wastewater: A review. *J. Environ. Chem. Eng*., 9(4), 105688. https://doi.org/10.1016/j.jece.2021.105688.
Sharma, A. K., Thornberg, D., Andersen, H. R., 2013. Application of waterworks sludge in wastewater treatment plants. Int. *J. Environ. Sci. Technol.*, 10(6), 1157-1166. https://doi.org/10.1007/s13762-012-0164-8.
Shen, Y., Wu, B., Wang, Y., et al., 2024. Temporal and spatial laws and simulations of erosion and deposition in the Lower Yellow River since the operation of the Xiaolangdi Reservoir. *J. Geogr. Sci.*, 34, 591–609. https://doi.org/10.1007/s11442-024-2219-x.
Shrestha, S., Kulandaivelu, J., Sharma, K., Jiang, G., Yuan, Z., 2020. Effects of dosing iron- and alum-containing waterworks sludge on sulfide and phosphate removal in a pilot sewer. Chem. Eng. J., 387, 106987. https://doi.org/10.1016/j.cej.2020.106987.
Song, S., Gong, Y., Yu, Y., 2024. Integrating pattern, process, and function in urban landscape ecological network planning: A case study of Harbin central city. Ecol. Indic., 159, 111671. https://doi.org/10.1016/j.ecolind.2024.111671.
Sun, N., Yao, Z., Xie, Y., Wang, T., Yang, J., Li, X., Fu, Q., 2023. Sustainability analysis of the water environment carrying capacity of Harbin City based on an optimized set pair analysis posture-deviation coefficient method evaluation model. Water, 15(8), 1575. https://doi.org/10.3390/w15081575.
Virkki, V., Alanr, E., Porkka, M., Ahopelto, L., Gleeson, T., Mohan, C., et al., 2021. Environmental flow envelopes: quantifying global, ecosystem–threatening streamflow alterations. Copernicus GmbH. https://doi.org/10.5194/hess-25-5649-2021.
Wang, F., Wei, D., Chen, M., Peng, S., Guo, Q., Zhang, X., et al., 2022. A synthetical methodology for identifying priority pollutants in reclaimed water based on meta-analysis. J. Environ. Sci., 112, 106-114. https://doi.org/10.1016/j.jes.2021.10.017.
Wang, G., Wang, L., Bohu, T., Gu, L., He, B., Zhang, H., et al., 2024. Deciphering microbial assembly and coexistence in rivers subjected to long-term reclaimed water replenishment. Environ. Pollut. 363(Pt 2), https://doi.org/10.1016/j.envpol.2024.123210.
Wigginton, N. S., 2016. Reclaimed costs from reclaimed water. Science, 352(6287), 784. https://doi.org/10.1126/science.aaf5664.
Zhang, W., Zhou, P., Pan, S., Li, Y., Lin, L., Niu, L., Wang, L., Zhang, H., 2022. The role of microbial communities on primary producers in aquatic ecosystems: Implications in turbidity stress resistance. Environ. Res., 215(Pt 1), 114353. https://doi.org/10.1016/j.envres.2022.114353.
Zhang, X., Xu, K., Zhang, D., 2012. Risk assessment of water resources utilization in Songliao Basin of Northeast China. Environ. Earth Sci., 67, 1319–1329. https://doi.org/10.1007/s12665-012-1575-5.
Zhao, P., Hu, Y., Ma, M., Wu, W., Xiao, J., 2022. Comparative study on international standards of reclaimed water quality for irrigation. SSRN Electron. J. https://doi.org/10.2139/ssrn.4245678.

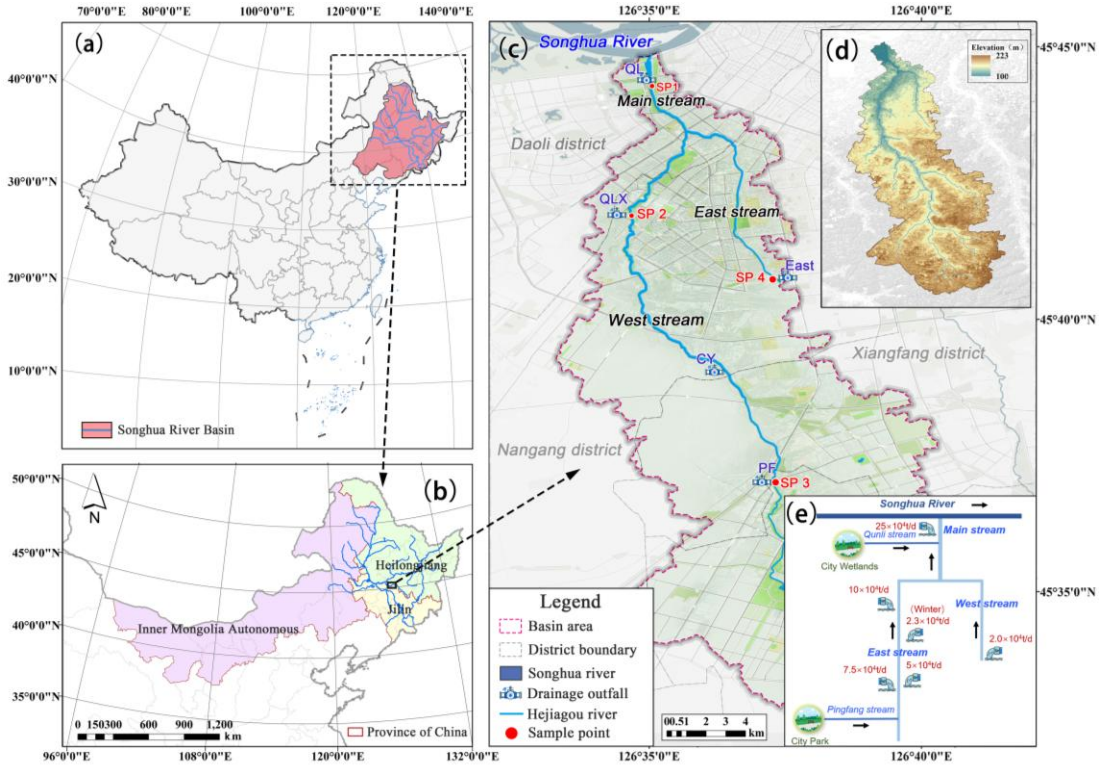


Fig.1. The study area map illustrates the geographical location of the RHJ watershed: (a) The Songhua River basin in northeastern China. (b) The Songhua River basin spans three provinces—Inner Mongolia, Jilin, and Heilongjiang—with RHJ situated in the central part of the basin within Heilongjiang Province. (c) The RHJ basin is situated in central Harbin, the provincial capital, on the south bank of the urban section of the Songhua River. It spans four districts and comprises the main stem, West Gully, and East Gully, with four monitoring points (SP1 (OF1), SP2 (OF2), SP3 (OF3) and SP4 (OF4)). (d) The watershed slopes from south to north, with elevations ranging from 100 to 223 meters. (e)Locations and flow rates of water outfall along the RHJ basin, along with minor tributary locations.

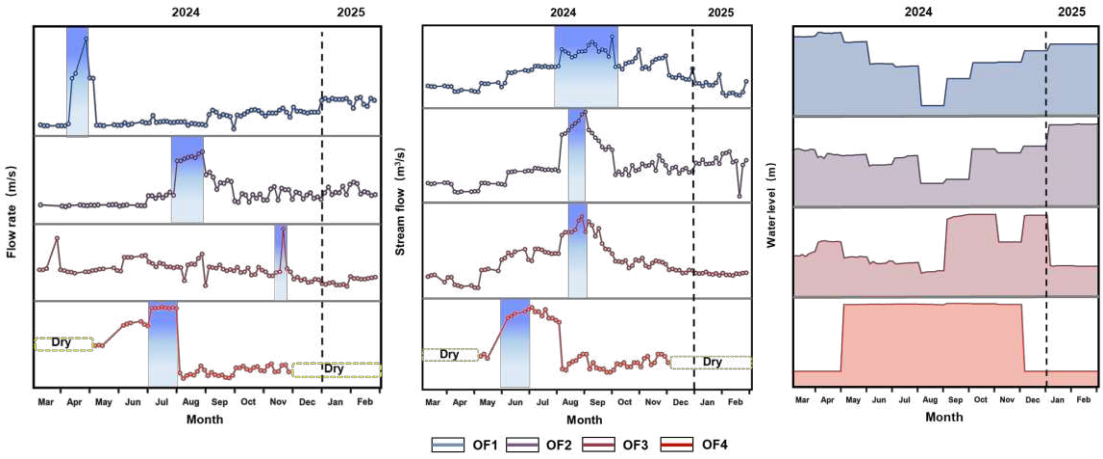


Fig.2 Monthly variations in hydrological data at four outfalls in RHJ basin

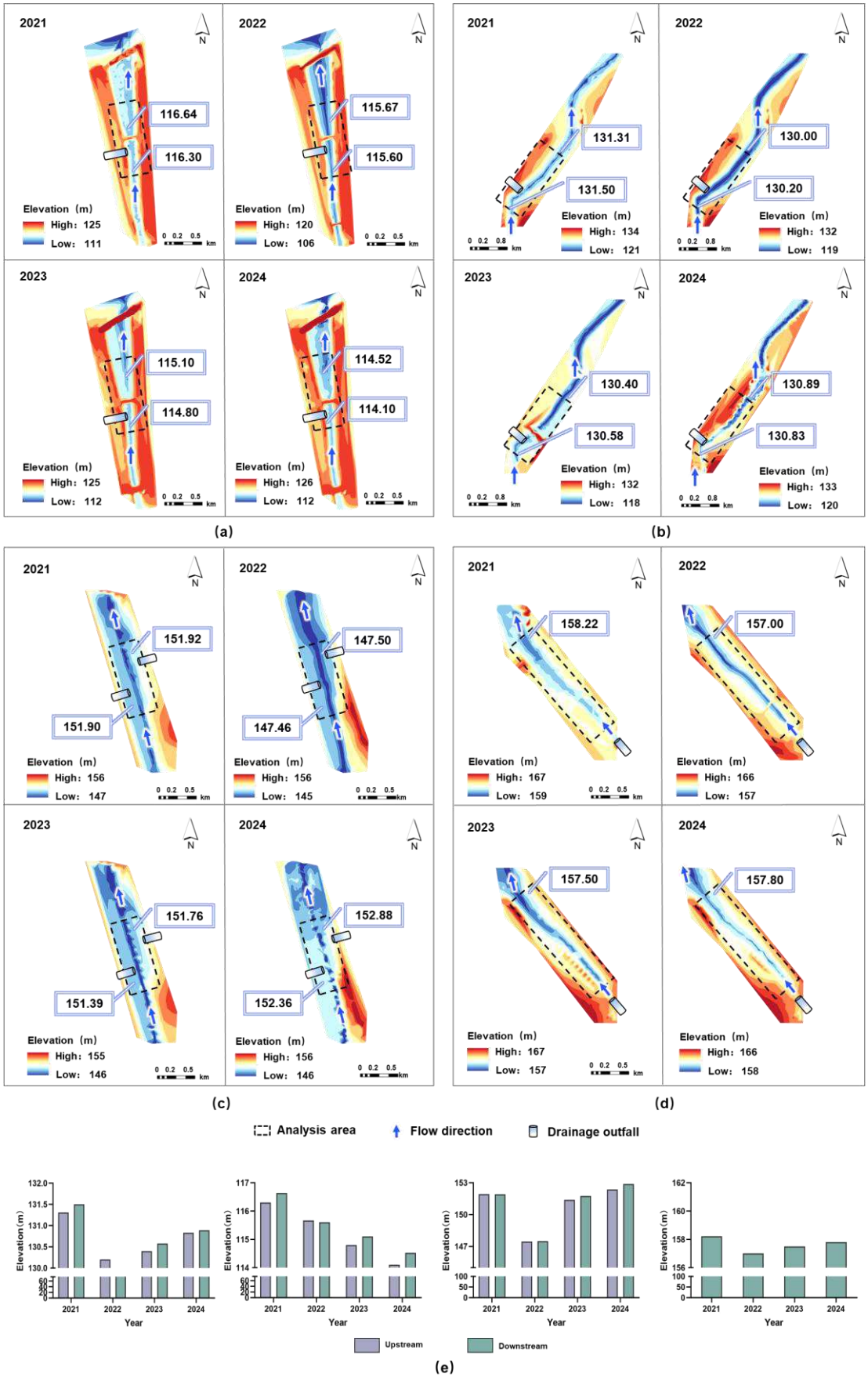


Fig.3. Annual analysis of topographic evolution upstream and downstream of four outfalls

in the RHJ basin.（a）OF1:AK0+400~AK1+000.（b）OF2:BK3+100~BK3+330.（c）OF3:BK25+000~BK28+000.（d）OF4:BK6+100~BK6+630.（e）Quantitative bar chart

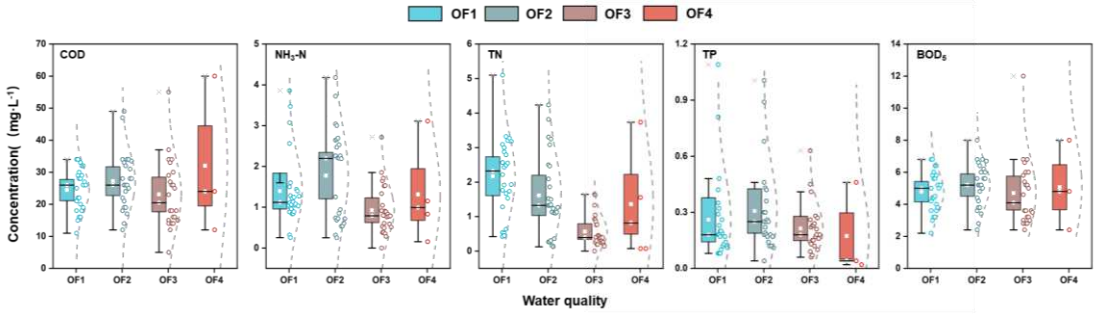


Fig.4. Monthly variations in water quality at four outfalls in RHJ basin

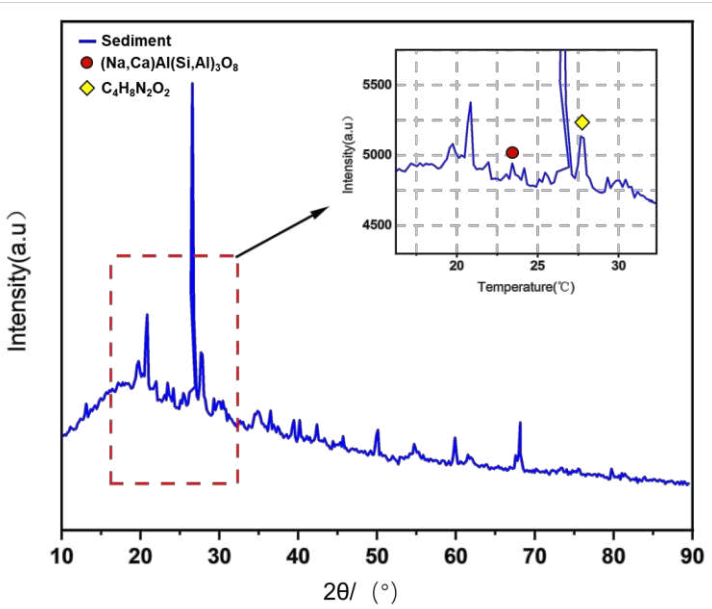


Fig.5. X-ray Diffraction analysis of riverbed sediments at the OF1

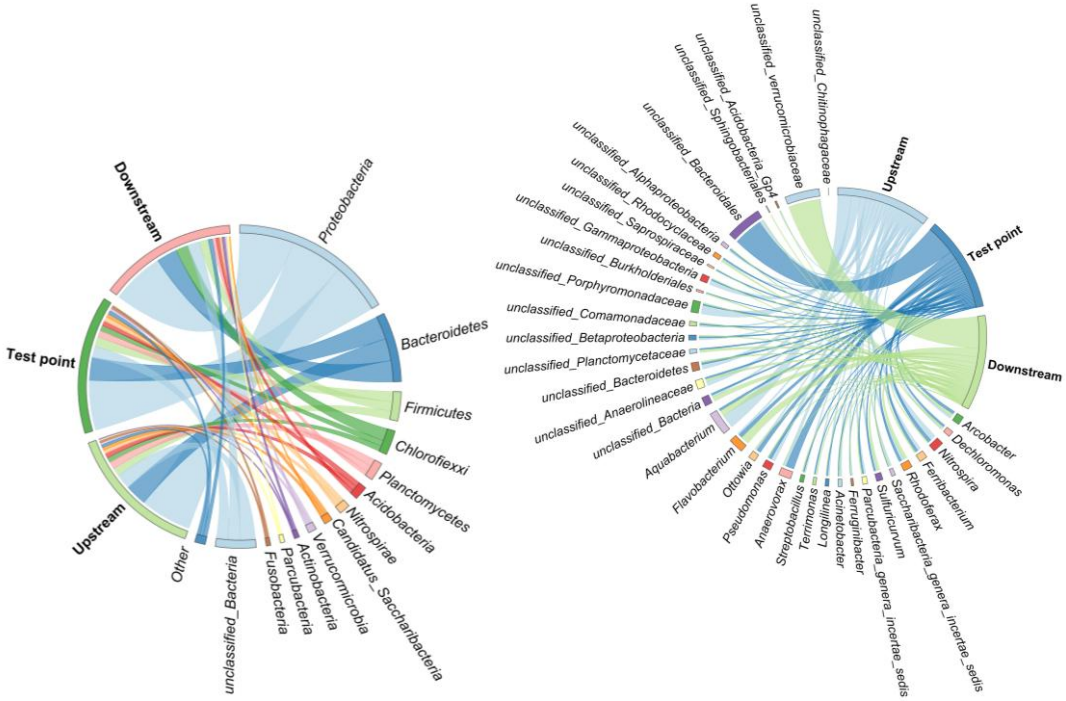


Fig.6. Microbial abundance at the phylum (genus) level at upstream, test point and downstream locations in sediment

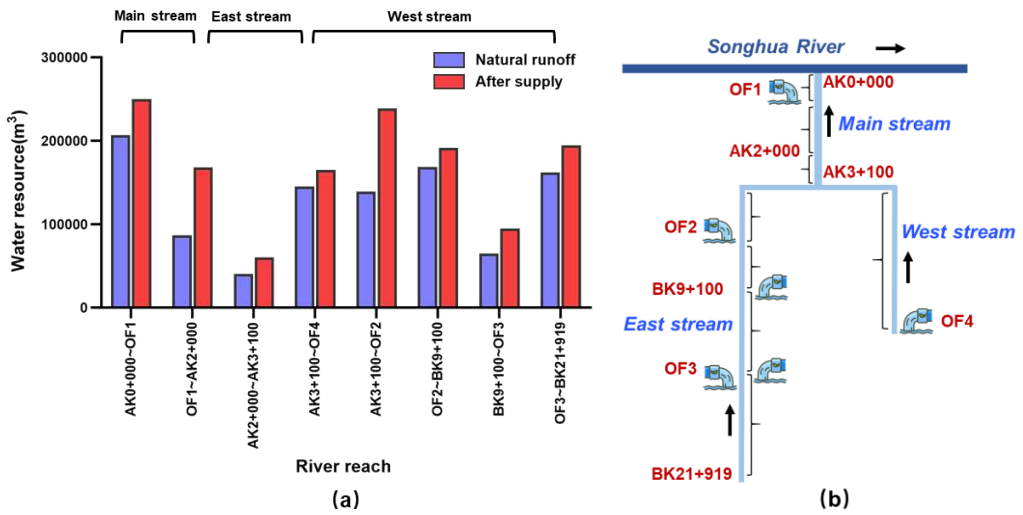
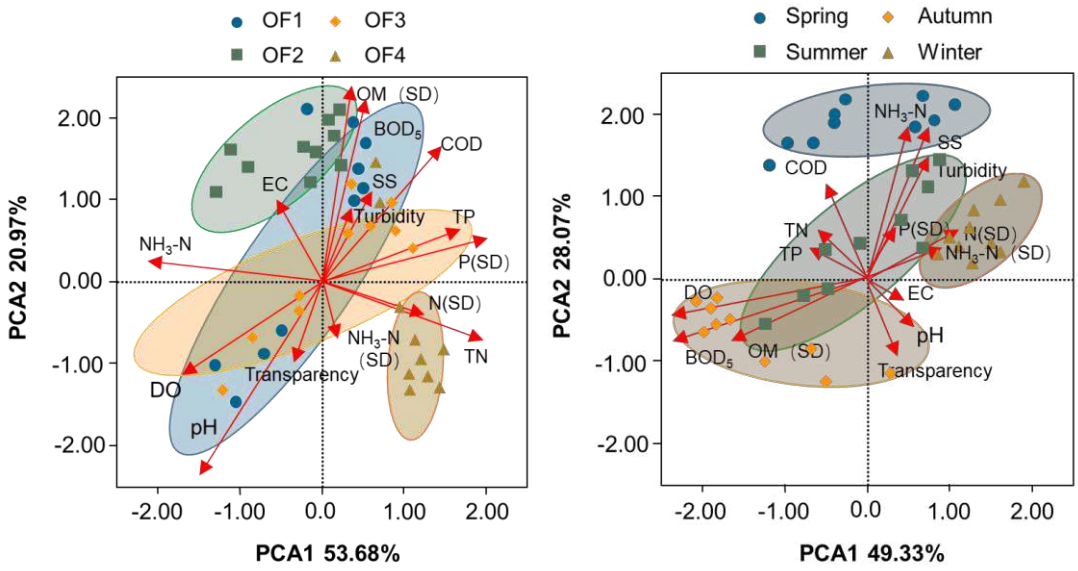


Fig.7.（a）Changes in total water resources.（b）River basin segmentation



（a） （b）

Fig.8.（a）PCA analysis separately explains the spatial variation in water pollutants and organic pollutants in sediments (SD),（b）the correlation between the OF1 discharge point and changes in water quality and sediments under different seasonal conditions.

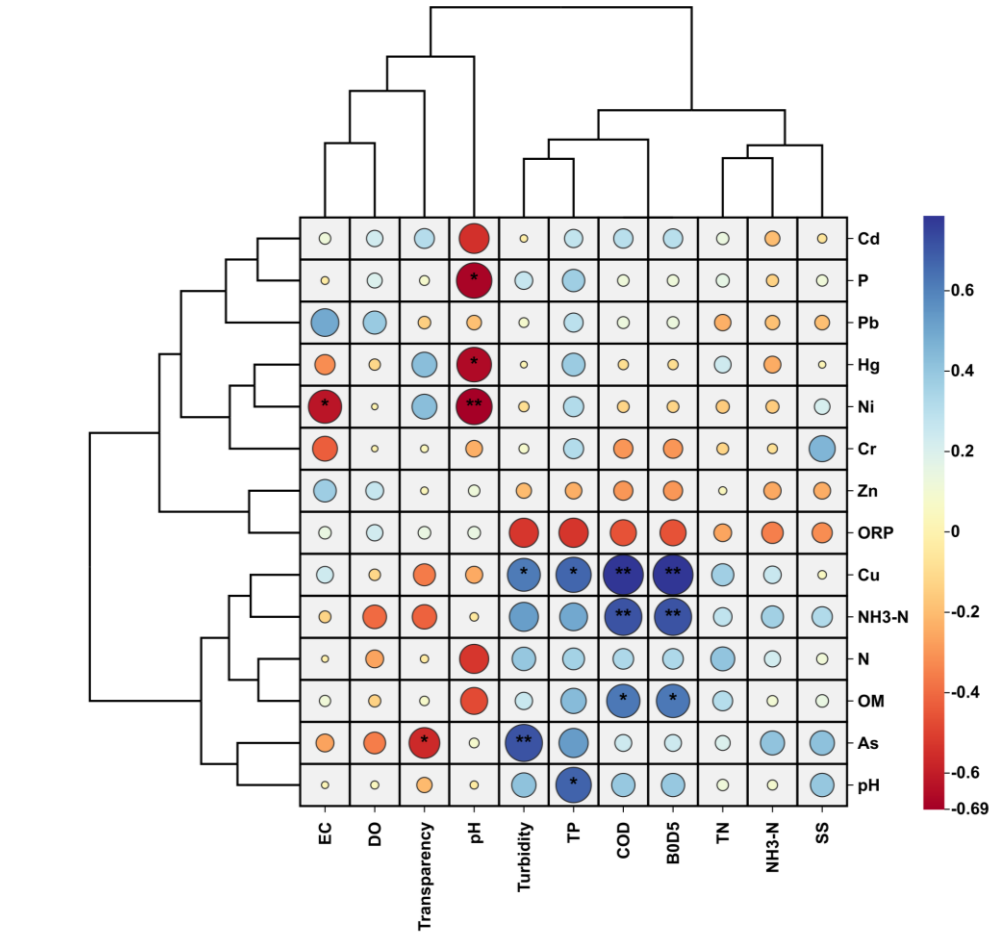


Fig.9. Correlation analysis between water quality at the OF1 outlet and heavy metal and organic compound levels in sediments in 2024 warm and cold colors represent positive and negative correlations.

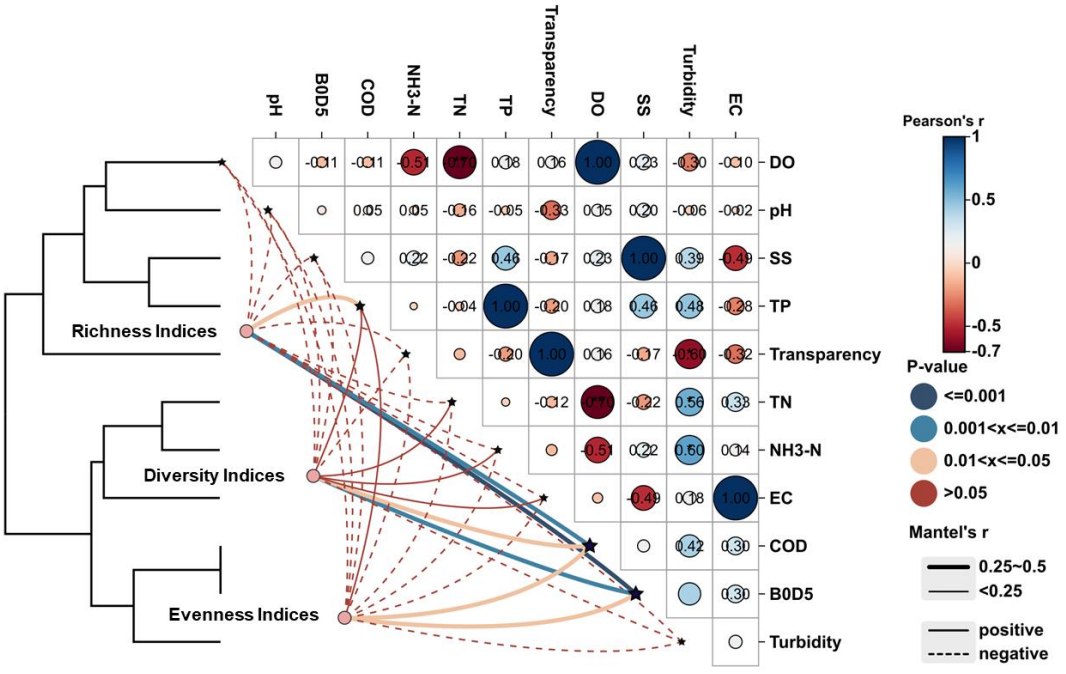
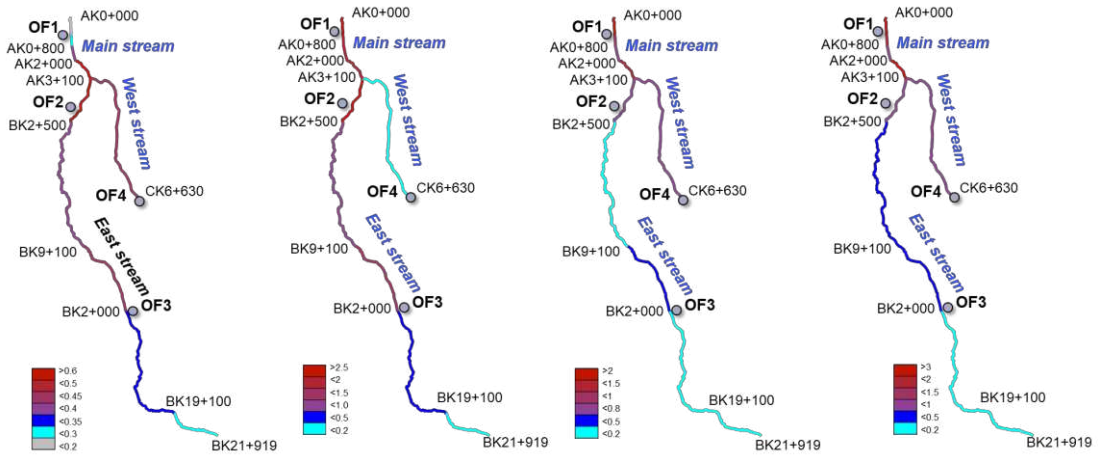


Fig.10. Correlation analysis between microbial diversity Indices at the OF1 outlet and water

quality parameters. Mantel tests. Edge width corresponds to the Mantel's r statistic for the corresponding distance correlations. And edge color denotes the statistical significance based on 9.999 permutations.



(a) (b) (c) (d)

Fig.11. Impact of the outfall on hydrological, hydrodynamic and water quality conditions in different sections of the RHJ basin. (a) Flow rate. (b) Flow velocity. (c) Scour depth. (d) Water quality, taking NH_3-N as the analytical factor

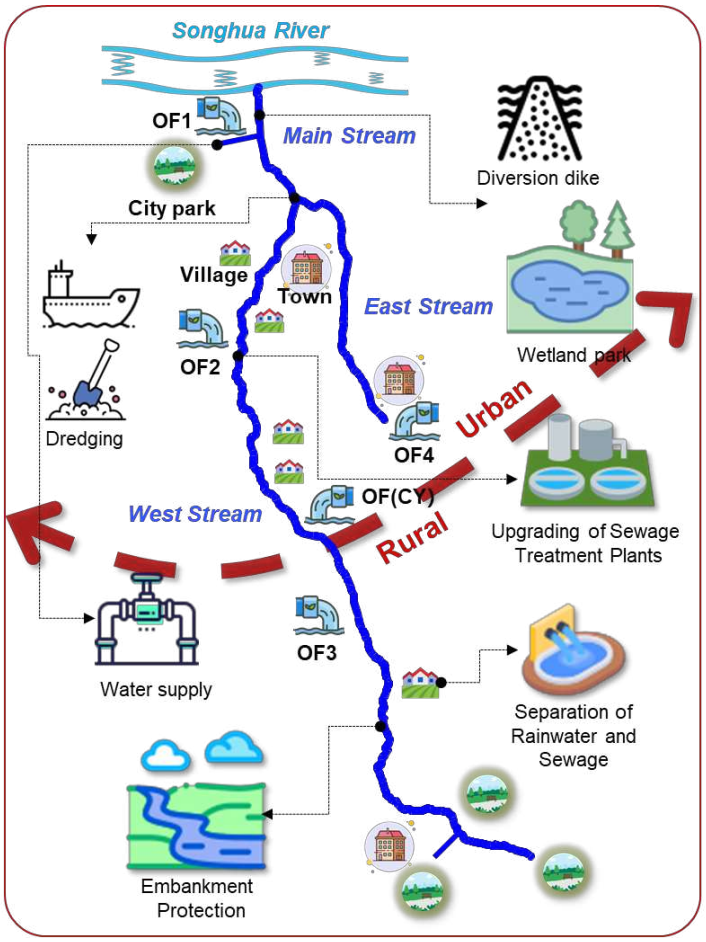


Fig.12. Comprehensive water environment management strategies for the RHJ basin to the characteristics of discharge-supplemented urban river

Supplementary Files

This is a list of supplementary files associated with this preprint. Click to download.

- Tables.docx